Research Article

A non-dispersive approach for a Raman gas sensor

L. Cocola[1] · G. Tondello[1] · L. Poletto[1]

Abstract

Although Raman spectroscopy is widely used on solids and liquids, its application on gaseous samples is far less commonplace due to technical issues related to dealing with very weak signals over a strong background. A demonstration of a possible approach for a simple, noninvasive Raman-based gas detector is presented and evaluated. This setup is meant to perform nitrogen and oxygen gas concentration measurements through Raman scattering working with optical filters instead of the traditional spectrograph and a lighting-grade 532 nm diode-pumped solid state laser as the pumping source. An industrial-grade CMOS camera is used as the detector, taking full advantage of the low noise and spatial resolution of this device. The system has been tested for both oxygen and nitrogen in a gas flow cell. Nitrogen measurement in a glass vial is reported in order to demonstrate and show some of the advantages that could be obtained with the use of an imaging detector instead of a single pixel one. The reported measurements show that even without using a dispersion spectrometer, this approach enables an indicative, noninvasive gas detection through glass vials with significant rejection of the elastic scattering contribution.

Keywords Raman · Gas sensing · Non dispersive · Imaging · Bandpass filter · Non invasive detection

1 Introduction

Raman spectroscopy is a well-developed analytical method that finds application both in the scientific as well as industrial domain [1]. Raman spectroscopy has the advantage of showing a characteristic spectrum of molecules, either rotational and/or vibrational, shifted into a portion of the visible spectrum enabling simultaneous measurement of different species while avoiding the technical complications of traditional infrared spectroscopy, which requires a very wide spectral region to be sounded. Also Raman spectroscopy can detect homonuclear molecules like H_2, N_2, O_2 that are non-active in absorption. On the other hand, Raman cross sections are very small compared to absorption cross sections for the same molecules, resulting in weak signals to be measured [2]. For this reason, commercial Raman sensing is already at an advanced state for detection and analysis of matter at solid and liquid phases [3, 4]. On the contrary, Raman gas sensors are less commonplace mainly due to the lower molecular density. Several solutions have been proposed for weak signal enhancement in gas detection, such as using high-power pumping sources and/or applying several kinds of optical enhancement techniques (optical coupled cavities, multi pass layouts, hollow fibers) [5–10]. Those techniques usually give a performance increase of several orders of magnitude, but unfortunately they are not applicable for noninvasive sensing through the material of a container. Among already developed Raman gas sensors based on an optical cell containing the gas under analysis and a dispersive spectrometer, we note the applications to fuels and gas composition analysis [11–15]. Data from the literature [16] can provide an interesting overview about the ultimate sensitivity performance which can be reached with state-of-the-art components and a single-pass optical cell

✉ L. Cocola, lorenzo.cocola@cnr.it | [1]National Research Council, Institute for Photonics and Nanotechnologies, Via Trasea 7, 35131 Padua, Italy.

coupled with a dispersive spectrometer; for both nitrogen and oxygen, this is in the hundreds of ppm range.

Main components of all these Raman systems are: the laser source that provides the exciting photons, a spectrograph for dispersion and the corresponding detector for spectral analysis. Usual requirements for the laser are its narrow spectral band (of the order of a small fraction of nm) and the stability of the emitted wavelength, although all those requirements can be relaxed depending on the particular application. Regarding the spectrograph, both dispersive [17] and Fourier transform types [18] are used in the literature. The latter type, particularly in the static heterodyne version, lends to miniaturization without compromising spectral resolution [19–21]. About detectors, both CCD or CMOS are used, usually operating with cooling devices to increase their sensitivity for the detection of small signals. For all these reasons, a gas-dedicated Raman system is a rather complicated and expensive device, not well suited to low-cost industrial applications.

A non-dispersive Raman (NDR) system uses filters instead of a spectrograph for selecting the portion of the spectrum of interest for the detection, greatly simplifying the device. A NDR can have high luminosity, i.e., a high light gathering capacity for the very weak Raman signal, a characteristic that is particularly useful for gas Raman sensing. Since the detectable spectral band is anyway limited by the spectral width of the filter, of the order of few nm, there is no advantage in using a narrow band laser any more: A simple laser diode is sufficient, with high optical power, high reliability and very low cost, such as the typical lighting grade devices used in projectors and light shows.

Compared with the traditional dispersive or Fourier transform spectroscopy, this approach is however only suitable for sensing simple mixtures composed of few gases such as the main components of ambient air (oxygen, nitrogen, water vapor) or similar mixtures as long as they have well-separated Raman lines, such as to fall in well-separated spectra regions.

NDR Raman sensing is already used in remote-sensing atmospheric devices, where high-power pulsed laser sources are used for LIDAR-type setups, enabling spatial-resolved sensing with a time-of-flight detection. In those contexts, the most common approach is to detect Raman scattered signal with non-dispersive spectroscopy allowing the use of fast, high gain detectors such as photomultiplier tubes or avalanche photodiodes coupled with time-tagging electronics [22, 23].

In the present work, we show the possibility of building a simple, compact, noninvasive and low-cost device as a detector for measuring the concentration of O_2 and N_2 in atmospheric air by applying NDR. These two molecules have their most pronounced vibrational Raman signature

(Q branch) well separated from each other (a necessary situation for NDR). In particular, a NDR-based device for N_2 detection using the Raman line at 2331 cm^{-1} could be of great interest as the only noninvasive, contactless optical method to detect this molecule that, being homonuclear, is absorption inactive. Oxygen and water vapor could be similarly detected with their Raman lines at 1555 cm^{-1} and 3654 cm^{-1}, respectively.

The implementation of the technique for noninvasive nitrogen detection inside vacuum-sealed pharmaceutical vials containing dried products could be used as an indicative testing method for seal leakage. This is also considered and demonstrated as a proof of principle and a possible application.

2 Materials and methods

2.1 Measurements on cell

The first tests were performed with sample gas contained in an enclosed cell, with optical windows and an integrated laser focusing lens.

Figure 1 shows the schematic of the experiment. The laser used here is a lighting-grade 532 nm, doubled Nd:YAG, TEC cooled Diode Pumped Solid State Laser (DPSSL) with a maximum power of 2 W (Lasever, LSR532H). The laser is focused with a 75 mm focal length aspheric lens with AR coating optimized for 532 nm and is linearly polarized.

The Raman signal is collected at 90° with respect to the laser direction and the plane of collection, i.e., the plane of the drawing in Fig. 1 is perpendicular to the laser field electric vector in order to maximize the collected Raman signal. Figure 2 shows the actual gas interaction cell.
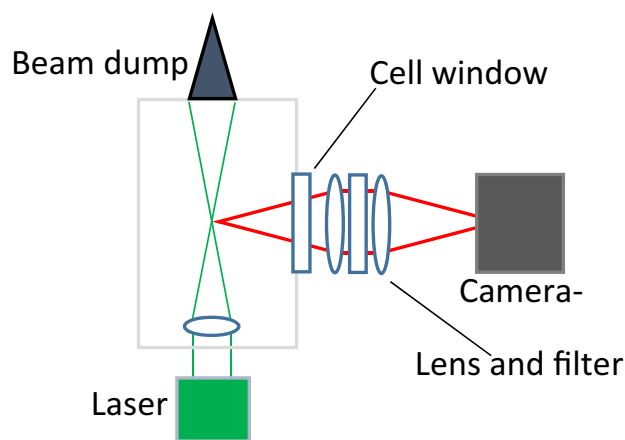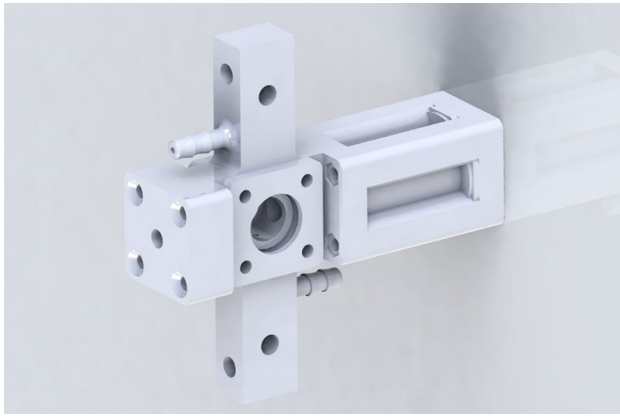

Fig. 1 Schematic of the experiment

Fig. 2 Gas cell assembly: 3D-printed nylon parts. Pump laser travels from right side (focusing lens seat) to left side (hole for copper pipe laser trap); Raman signal is collected from front window

Fig. 3 Example camera image, showing a detail of the three ROIs in yellow [l, r (sides up and down): reference, c (center): Raman signal]

The traditional approach in non-dispersive Raman spectroscopy is to split the collected light in two parts and use two filters, one in-band for each sensing wavelength and one or more out-of-band, followed by different single detectors: This is done to compensate against spurious light such as stray light or residual Rayleigh-scattered light diffused from the surroundings. We chose to use only the in-band filter instead, one for the O_2 line at 580 nm, one for N_2 at 607 nm. The filters used are from Edmund Optics, centered at 580 nm and 610 nm for O_2 and N_2 lines, respectively, with nominal FWHM of 10 nm and blocking OD of four. With the use of dichroic mirrors, simultaneous sensing of the different gases could be possible. The compensation is done instead by forming the image of the region near the focus of the laser on a camera through a couple of $f = 24$ mm, $d = 23$ mm aspheric lenses (working in 1:1 magnification). The bandpass filter is placed in between the lenses (as the filter is designed to work with collimated light at normal angle of incidence) to remove the Rayleigh component; an additional colored plastic filter is used to improve rejection of stray light impinging with far from normal angle of incidence.

Unlike other setups using the non-dispersive approach, where a single-pixel detector is used to acquire the Raman filtered signal, we use a 2D detector in order to be able to distinguish in the same image the useful signal and the background to be subtracted, as explained later. A compact and low-cost industrial-inspection-type camera is used, operated at room temperature (Basler, aca1920-40gm). It has a dark noise of 6.7 electrons and about 60% quantum efficiency at the wavelength of the nitrogen line. The sensor size is 11.3 mm × 7.1 mm with a 5.68 μm pixel pitch. A notable advantage related to the use of an imaging sensor instead of multiple detectors comes from the easier alignment procedure. After an initial coarse
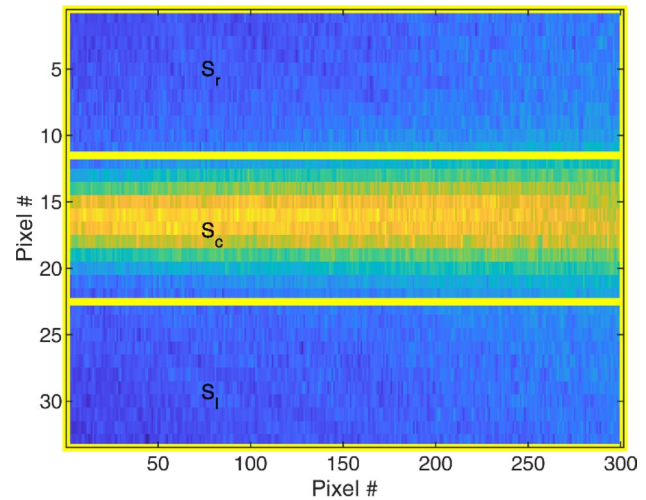
adjustment, the fine tuning of the alignment can be performed via software, by properly shifting the different ROIs, which are sized 1430 μm along the beam propagation and 164 μm in the transverse direction each. Figure 3 shows the N_2 line taken with ambient air in the cell and 2 s of exposure with such a camera. Three Region Of Interest (ROIs), as shown in Fig. 3, are then integrated on the camera by summing the pixel counts. In other words, the compensation channel is realized spatially on the image instead of spectrally.

The final measurement is $S_c - (S_l + S_r)/2$, with S being the sum of pixel counts within a ROI. All the measurement frames were dark-corrected by subtracting a dark frame recorded at the beginning of the measurement process with the pump laser turned off.

An important feature of the use of the two external ROIs for compensation (i.e., S_l and S_r) is the intrinsic compensation against possible drifts of the dark-count level which is typical of passively cooled, industrial-grade cameras.

No normalization for the pump power is used in the processing procedure. Indeed, it has been verified that the standard deviation of the signal on images integrated on 2 s even for 1 h acquisition time is slightly worse when the normalization is applied. This means that the stability of the laser emission is not the limiting factor in the sensitivity.

Previous tests done with a scientific-grade cooled camera (PCO, Sensicam) did not show significant improvements in the signal-to-noise ratio compared to the images acquired with the industrial-grade camera. The main noticeable effect is a remarkable dark-count drift of the industrial-grade camera frames during the first measurements after system startup, due to the temperature rise

of the detector board. However, this effect is negligible after the camera has reached its operating temperature, which happens after running the acquisition procedure for a couple of minutes.

2.2 Measurements on vials

As a proof of principle, the application of this technique to pharmaceutical vials (such as in Fig. 4) for the detection of nitrogen has been demonstrated. Such a measurement can be relevant for testing the closure tightness of pharmaceutical products which are sealed in an oxygen-free, modified atmosphere. The optical setup has been slightly changed for this particular case: To increase spot size at the glass surface and to minimize any risk of damage to the glass, the focusing lens was changed to a 30 mm focal length. The collection area defined in the processing software was kept the same: Although the shorter laser focal

length would theoretically result in a smaller focus spot, however, due to additional distortions, shifts and aberrations introduced by the vial glass, no reduction of the spot size has been observed.

Although apparently clear, the vial glass shows tiny defects (such as diffusion centers and vertical stripes) which become noticeable under the illumination of the strong pump light. If the laser beam is directly hitting some of those defects, a strong diffusion is observed. In some cases, the spectrum of the diffused light is not even elastic, but a fluorescence component is present. This becomes apparent while viewing the illuminated vial through laser safety goggles; in some cases an illuminated "orange ring" appears all around the vial at the laser-to-glass interaction height. This emission is explained as a combination of fluorescence effect and light guiding provided by the geometry of the vial. Oxygen sensing proved to be particularly unstable for those reasons, intuitively because the 580 nm Raman line is closer to the pump.

An example of an acquired frame (for ambient air) is provided in Fig. 5. The processing of those data required a more careful approach, as described in the Results and discussion section.

3 Results and discussion

3.1 Measurement on cell

Here are presented some results obtained with the cell configuration, as a test for stability, reproducibility, minimum detectable concentration and crosstalk for oxygen and nitrogen. Figure 6 shows the signal obtained with an integration time of 2 s when the cell is filled with a mixture of O_2 and N_2 at various concentrations of the two keeping

Fig. 4 Typical clear, 22-mm-dia. tubular glass vial
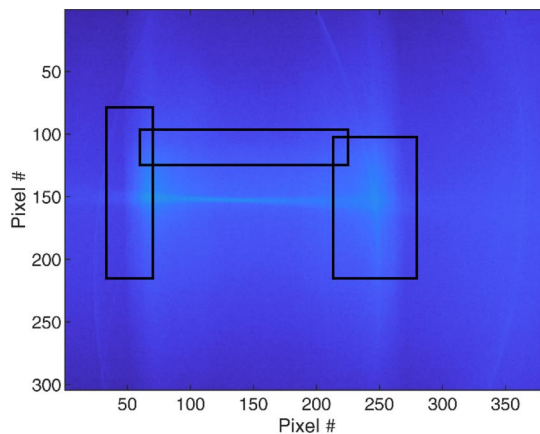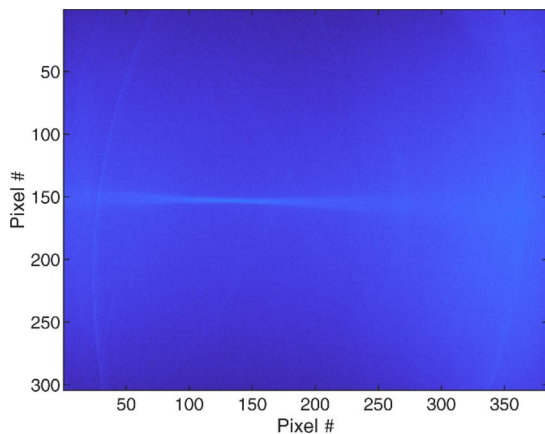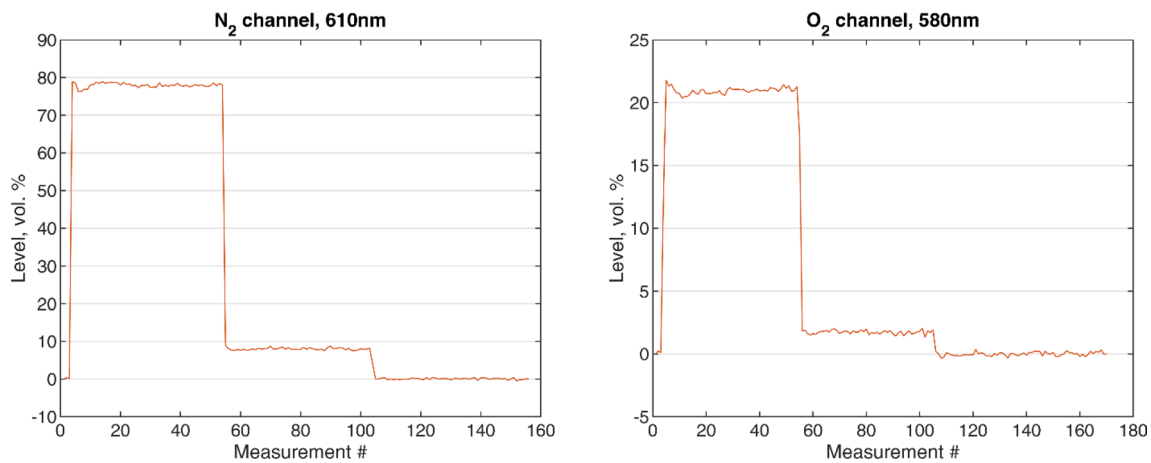

Fig. 5 Example of a typical "good" frame (left) and noisy frame (right) acquired through the vial, showing some diffusion, reflection and fluorescence artifacts (marked with black boxes) which

appear in the noisy frame as a non-uniform background lighting. For the effect on the actual measurement, see Fig. 7

Fig. 6 Measurements on three different levels (Table 1) for nitrogen (left) and oxygen (right)

Table 1 Performance evaluation of the measurement

	(1) Air	(2) Mix	(3) Zero	Calibration (a.u.)/vol%
Nitrogen				
Measurement #	10–54	57–102	106–151	0.83
Mean (a. u.)	64.7	6.6	0.1	
SD (a. u.)	0.4	0.2	0.2	
SD (vol. %)	0.4	0.3	0.2	
Oxygen				
Measurement #	15–54	56–105	108–165	1.88
Mean (a.u.)	39.5	3.3	0.0	
SD (a.u.)	0.4	0.3	0.3	
SD (vol%)	0.2	0.2	0.1	

The calibration factors are obtained by assuming 78% N_2 and 21% O_2 in air

the total pressure constant at ambient level. Three concentration levels have been tested with each gas:

1. ambient air level (which is assumed to be 78% for nitrogen and 21% for oxygen within the scope of this work); note that the initial transient is due to pump laser being turned on;
2. roughly 1/10 of ambient level, with the use of a "displacement" gas metered through needle valves. Carbon dioxide was used for diluting ambient nitrogen for safety reasons as the cell and metering system is not oxygen-clean; note that carbon dioxide has a strong Raman emission close to the oxygen line, therefore it does not influence the measurements of the nitrogen content. This proved to be true by measuring actual values around zero when the cell was flushed with carbon dioxide. Nitrogen was used instead as a dilution gas for oxygen;

3. zero level, corresponding to the signal acquired with the cell flushed with 100% dilution gas.

The average measurement obtained in ambient air was used to calculate the calibration coefficient and to scale the standard deviation values in concentration units.

The limit of detection (LOD) obtained in the cell is calculated from the standard deviation measured on the signal when the cell is flushed with dilution gas and is assumed to be three times the standard deviation, resulting in 0.6 vol% nitrogen and 0.3 vol% oxygen. Due to the intrinsic linearity of both the Raman effect, the detector and the processing software, the noise level can be already considered an indication of the LOD. The simplest way to increase the LOD is to act on the integration time of the camera, depending on the measuring time required by the experiment.

3.2 Measurement on vial

Tests on vials required a peculiar approach due to the large amount of light scattered by the glass material and the presence of optical defects. In order to make several measurements through different portions of the glass vial, the sample was rotated during the acquisition. The vial was placed on a rotation stage with a rotating speed of one turn per 130 s. The acquisition time was set at 2 s, therefore 65 images have been acquired for a full 360-degree turn. Given the rotation speed and acquisition frame rate, the vial can be considered almost stationary during a single measurement.

The vial was tested with only (1) ambient air or (2) carbon dioxide purging. The neck of the vial was open during the measurements, with a purging gas pipe blowing through the upper part of the vial.

After the same image processing technique used on the cell was applied to the collected data, it became apparent that some of the frames were tainted by an excess of diffused fluorescence. This happens when the laser beam hits a bad spot on the glass.

A strategy to identify and discard those frames was however found. This can be done by calculating the unbalance between the two reference ROIs: $q = |2*(S_l - S_r)/(S_l + S_r)|$. This unbalance parameter q can be used as an indication of optical measurement quality. This is shown in Fig. 7. For the experiment, all the measurements with q values exceeding 0.01 have been discarded, resulting in 20% unusable images with the vial in air (65 images over 324) and 12% unusable images at zero level (36 images over 295).

With respect to the tests on the cell, where the LOD for nitrogen has been found to be 0.6% concentration, many disturbances on the acquisition are introduced due to the lower optical quality of the glass in vials. The resulting LOD is 2.7% nitrogen concentration (calculated as three times the standard deviation), four to five times worse than the cell (Table 2).

At present, leakages in vials are detected through Tunable Diode Laser Absorption Spectroscopy (TDLAS), that measures the internal concentration of oxygen as a signature of possible leakages of the seals. TDLAS is operated on the very weak O_2 lines at 760 nm [24]. State-of-the-art sensors for industrial applications have standard deviations of 0.2–0.3 vol% oxygen [25]. For micro-leak testing, containers are stored for a defined amount of time to allow seepage from the minimum detectable leak to reach a fixed
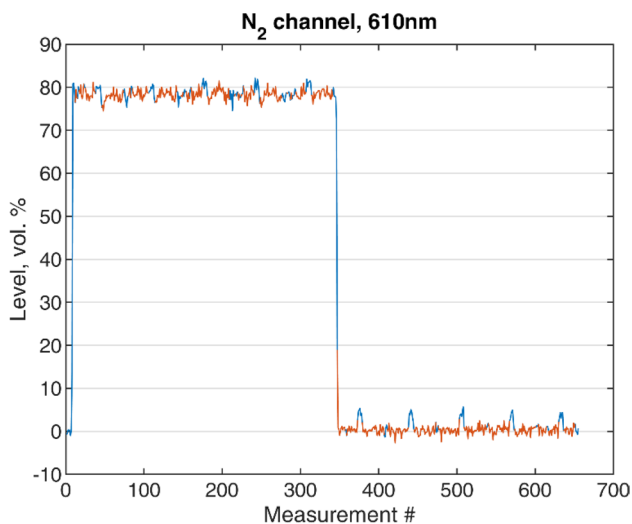
Table 2 Performance evaluation of the measurement

Nitrogen	(1) Air	(2) Zero	Calibration (a.u.)/(vol%)
Measurement #	18–341	354–648	1.33
Mean (a. u.)	104.4	0.4	
SD (a. u.)	1.5	1.1	
SD (vol. %)	1.1	0.9	
Measurement count	324	295	
Measurement failure	65	36	

level. The better the sensitivity of the tester instrument is, the faster the process of analysis can be performed.

The NDR detection is performed on nitrogen, that is a factor ≈4 in volume concentration compared to oxygen in air. The standard deviation of the present device of about 1 vol% nitrogen is equivalent to 0.25 vol% oxygen for the purpose of detecting an ambient air leak inside an evacuated container. Therefore, the LOD with the NDR technique is comparable to the LOD with TDLAS-based sensors. Furthermore, the complexity and cost of the proposed device is certainly much less than a TDLAS-based sensor. Finally, a remarkable simplification using NDR technique is the total insensitivity to the external atmosphere, since the Raman emission that is detected takes place inside the container. Indeed, TDLAS-based sensors are sensitive to the total optical path of the laser from the source to the detector, including the path in external air; therefore, the unwanted absorption given by the oxygen outside the vial has to be taken into account, either by minimizing the external path or keeping the instrument in nitrogen flux. Therefore, the geometry and complexity of a NDR-based sensor are much more simple than a TDLAS-based one.

4 Conclusions and future developments

The measurements on cell show that non-dispersive Raman can be used as a simple indicative method to evaluate nitrogen and oxygen concentrations in air or simple gas mixtures (assuming that no interfering components are present). This can be useful for air and most breathable mixtures as an alternative to more complex and invasive nitrogen and oxygen sensors. While oxygen may be sensed in the near infrared with tunable diode laser absorption spectroscopy, the case of nitrogen is particularly interesting as it does not exhibit infrared absorption, therefore requires invasive sensing methods such as mass spectrometry. For mixtures containing carbon dioxide, some kind of a sensor fusion approach may be investigated: For example, the ambiguity due to

Fig. 7 Repeated measurements on air and carbon dioxide purging for nitrogen channel. Orange shows data points that have been processed (with $q < 0.01$)

the overlap between oxygen and carbon dioxide Raman lines could be resolved by adding one of the many non-dispersive or TDLAS infrared sensors available on the market [26] as an independent carbon dioxide sensor.

The experiment on glass vial shows that the spatial subtraction method, only suitable if an image detector system, i.e., a matrix is used, can be useful for the rejection of diffusion and fluorescence light that is associated with the use of slightly irregular samples, or samples made of materials not properly meant for propagation of the high-power Raman pump.

Using a CMOS array instead of a single-pixel detector has two main advantages: the first being the availability of a low-noise and low-cost detector thanks to the on-chip measurement, the second being the spatial resolution which allows a range of smart software compensation techniques to overcome the typical limitations of the detection of weak Raman signals in the presence of a strong pump.

Moreover, data from an imaging sensor are suitable for the implementation of a range of techniques to allow rejection of measurements which are compromised by irregularities in the optical path. This feature could be used either to discard "failed" measurements or to find an optimal measurement spot (e.g., in the case of a sample with circular symmetry which can be rotated to avoid the presence of some sparse irregularities in the measurement path). Image data could also be averaged more and processed to improve sensitivity; anyway the way lower detection performance obtained on the vial seems to suggest that the main limitation is in the glass quality and fluorescence.

Using a much higher pump power could prove difficult as the heating and risk of damage to the glass vial becomes non-negligible; the possibility to use a simple, relatively broad-band and not temperature-stabilized laser, e.g., a simple diode, for Raman gas sensing should be exploited. In practice, the spectral band of the laser diode and its variation with the temperature must remain well within the FWHM of the filters used (in this case 10 nm). This requirement is relatively easy to satisfy, and most diode laser will match these specifications, some even feature an embedded reference photodiode for constant power operation minimizing output fluctuations. As an example, industry-standard diode lasers for lighting and engraving applications are available as OEM components and provide output power levels of several watts at 450 nm with a wall-plug efficiency above 30% and a 2 nm linewidth [27]. Those devices can be operated over a 5 nm range for a 50 °C temperature range.

Non-dispersive Raman analysis can be used as a compact, noninvasive and low-cost technique for the measurements of gas content in simple mixtures in close containers.

Compliance with ethical standards

Conflict of interest On behalf of all authors, the corresponding author states that there is no conflict of interest.

References

1. Paul R, Safa G, Dina G (2016) Raman spectroscopy, review. Int J Eng Technol Res 6:50–64
2. McCreery RL (2001) Raman spectroscopy for chemical analysis. Wiley, New York
3. Harris CM (2003) Raman on the run. Anal Chem. https://doi.org/10.1021/ac031242v
4. Mogilevsky G, Borland L, Brickhouse M, Fountain AW III (2012) Raman spectroscopy for homeland security applications. Int J Spectrosc. https://doi.org/10.1155/2012/808079
5. Hippler M (2015) Cavity-enhanced raman spectroscopy of natural gas with optical feedback CW-diode lasers. Anal Chem. https://doi.org/10.1021/acs.analchem.5b01462
6. Buldakov MA et al (2013) Analyzing natural gas by spontaneous Raman scattering spectroscopy. J Opt Technol. https://doi.org/10.1364/jot.80.000426
7. Yu A, Zuo D, Li B, Gao J, Wang X (2016) Parabolic cell for low-background Raman analysis of gas samples. Appl Opt. https://doi.org/10.1364/ao.55.003650
8. Buric MP, Chen KP, Falk J, Woodruff SD (2008) Enhanced spontaneous Raman scattering and gas composition analysis using a photonic crystal fiber. Appl Opt. https://doi.org/10.1364/ao.47.004255
9. Knebl A et al (2019) Fiber-enhanced Raman gas spectroscopy for 18O-13C-labeling experiments. Anal Chem. https://doi.org/10.1021/acs.analchem.8b05684
10. Sieburg A, Schneider S, Yan D, Popp J, Frosch T (2018) Monitoring of gas composition in a laboratory biogas plant using cavity enhanced Raman spectroscopy. Analyst. https://doi.org/10.1039/c7an01689a
11. Buldakov MA, Korolev BV, Matrosov II, Petrov DV, Tikhomirov AA (2013) Raman gas analyzer for determining the composition of natural gas. J Appl Spectrosc. https://doi.org/10.1007/s10812-013-9731-6
12. Kiefer J (2015) Recent advances in the characterization of gaseous and liquid fuels by vibrational spectroscopy. Energies. https://doi.org/10.3390/en8043165
13. Eichmann SC, Trost J, Seeger T, Zigan L, Leipertz A (2011) Application of linear Raman spectroscopy for the determination of acetone decomposition. Opt Express. https://doi.org/10.1364/oe.19.011052
14. Eichmann SC, Weschta M, Kiefer J, Seeger T, Leipertz A (2010) Characterization of a fast gas 2 analyzer based on Raman scattering for the analysis of synthesis gas. Rev Sci Instrum. https://doi.org/10.1063/1.3521397
15. Kiefer J et al (2008) Design and characterization of a Raman-scattering-based sensor system for temporally resolved gas analysis and its application in a gas turbine power plant. Meas Sci Technol. https://doi.org/10.1088/0957-0233/19/8/085408

16. Buldakov MA, Matrosov II, Petrov DV, Tikhomirov AA (2012) Raman gas-analyzer for analyzing environmental and technogenic gas media. Atmos Ocean Opt. https://doi.org/10.1134/S1024856012040057

17. Bell RE (2004) Exploiting a transmission grating spectrometer. Rev Sci Instrum. https://doi.org/10.1063/1.1787601

18. Egan MJ, Angel SM, Sharma SK (2017) Standoff spatial heterodyne Raman spectrometer for mineralogical analysis. J Raman Spectrosc. https://doi.org/10.1002/jrs.5121

19. Gomer NR et al (2011) Raman spectroscopy using a spatial heterodyne spectrometer: proof of concept. Appl Spectrosc. https://doi.org/10.1366/11-06298

20. Jennings DE, Weber A, Brault JW (2009) Raman spectroscopy of gases with a Fourier transform spectrometer: the spectrum of D2. Appl Opt. https://doi.org/10.1364/ao.25.000284

21. Bendtsen J, Rasmussen F, Brodersen S (2008) Fourier-transform instrument for high-resolution Raman spectroscopy of gases. Appl Opt. https://doi.org/10.1364/ao.36.005526

22. Wang L, Stanic S, Eichinger W, Song X, Zavrtanik M (2019) Development of an automatic polarization raman LiDAR for aerosol monitoring over complex terrain. Sensors (Switzerland). https://doi.org/10.3390/s19143186

23. Liméry A, Cézard N, Bertrand J, Hauchecorne A (2016) A multichannel Raman Lidar in photon counting mode using SiPM technology. Imaging Appl Opt. https://doi.org/10.1364/LACSEA.2016.LTh1G.4

24. Duncan DI, Veale JR (2004) Introduction to laser-based headspace inspection and the application to 100% container closure inspection of sterile pharmaceutical containers. Lighthouse Instrum. https://doi.org/10.1016/j.visres.2010.11.009

25. Jenkins TP, Berg T (2008) Diode laser absorption sensor for detecting oxygen in head space of vials. In: Proceedings of IEEE sensors. https://doi.org/10.1109/icsens.2008.4716432

26. Hodgkinson J, Smith R, Ho WO, Saffell JR, Tatam RP (2013) Non-dispersive infra-red (NDIR) measurement of carbon dioxide at 4.2 μm in a compact and optically efficient sensor. Sens Actuators B Chem. https://doi.org/10.1016/j.snb.2013.06.006

27. OSRAM Opto Semiconductor (2015) Blue laser diode in TO90 package PLPT9 450C

Publisher's Note Springer Nature remains neutral with regard to jurisdictional claims in published maps and institutional affiliations.